ACCEPTED MANUSCRIPT
Preprint typeset using LaTeX style emulateapj v. 2/19/04

SPITZER-IRS SPECTROSCOPY OF THE PROTOTYPICAL STARBURST GALAXY NGC 7714

B.R. BRANDL
Leiden University, P.O. Box 9513, 2300 RA Leiden, The Netherlands

D. DEVOST, S.J.U. HIGDON, V. CHARMANDARIS[‡], D. WEEDMAN, H.W.W. SPOON, T.L. HERTER, L. HAO, J. BERNARD-SALAS, J.R. HOUCK
Cornell University, Astronomy Department, Ithaca, NY 14853

AND

L. ARMUS, B.T. SOIFER, C.J. GRILLMAIR, P.N. APPLETON
Caltech Spitzer Science Center, 314-6, Pasadena, CA 91125
Accepted manuscript

ABSTRACT

We present observations of the starburst galaxy NGC 7714 with the Infrared Spectrograph *IRS*[1] on board the *Spitzer Space Telescope*. The spectra yield a wealth of ionic and molecular features that allow a detailed characterization of its properties. NGC 7714 has an H II region-like spectrum with strong PAH emission features. We find no evidence for an obscured active galactic nucleus, and with [Ne III] / [Ne II] ≈ 0.73, NGC 7714 lies near the upper end of normal-metallicity starburst galaxies. With very little slicate absorption and a temperature of the hottest dust component of 340 K, NGC 7714 is the perfect template for a young, unobscured starburst.

Subject headings: dust, extinction, galaxies: individual (NGC 7714, Arp 284), galaxies: starburst

1. INTRODUCTION

NGC 7714 is a peculiar barred-spiral galaxy at 45° inclination. For $cz = 2798$ km/s the galaxy is at distance[2] of 39.6 Mpc . Together with its post-starburst companion NGC 7715 it forms the interacting system Arp 284, which is the result of a recent ($100 - 200$ Myr), off-center collission between the two disk galaxies (Struck & Smith 2003). With its compact, UV-bright nucleus, NGC 7714 has been classified by Weedman et al. (1981) as the prototypical starburst galaxy. The central region of about 330 pc has been the site of active star formation at a rate of about $1 M_\odot\,\mathrm{yr}^{-1}$ for some 10^8 years. However, a recent significant increase in the star formation rate made it the dominating source of the UV flux (Lançon et al. 2001).

With its strong HeII λ4686 line (González-Delgado et al. 1995), NGC 7714 has been classified as a Wolf-Rayet galaxy. In fact, the optical and UV spectra indicate a population of about 2000 Wolf-Rayet and 20000 O-type stars, suggesting a fairly young age of the present starburst of $4 - 5$ Myr (Garcia-Vargas et al. 1997). This is in agreement with earlier studies by Weedman et al. (1981) and Taniguchi et al. (1988) who estimated 10^4 O5-type stars from the Balmer and Bracket-γ line fluxes, and masses of ionized gas of $3.0 \times 10^6 M_\odot$, and $1.9 \times 10^6 M_\odot$, respectively. The radio-continuum and the X-ray luminosity of 6×10^{40} ergs s^{-1} require 10^4 supernova remnants in a volume of radius 280 pc (Weedman et al. 1981). Taniguchi et al. (1988) found definite evidence for a starburst-driven bipolar winds from the nucleus, nearly perpendicular to the disk plane.

Although most of the activity is concentrated in the nucleus, NGC 7714 as a whole is experiencing intense star formation (González-Delgado et al. 1995). Mid-IR imaging with *ISOCAM* (O'Halloran et al. 2004) revealed a strong source at the nucleus surrounded by slightly extended emission out to about 30″ (5.7 kpc) in diameter. From the *IRAS* fluxes (Surace et al. 2004) and the above distance we calculate a total infrared luminosity of $L_{8-1000\mu m} = 5.6 \times 10^{10} L_\odot$.

The strong optical emission lines, Hβ and [O III], show no signs of broad emission (Weedman et al. (1981), Taniguchi et al. (1988)). Recently, Soria & Motch (2004) found two compact X-ray sources with *XMM-Newton*. One of them coincides with the starburst nucleus, has an X-ray luminosity of $L_X \approx 10^{41}$ erg s^{-1}, and shows the spectrum of a thin thermal plasma with a power-law (point-source) contribution. The variability in the power-law component hints at the presence of either a hidden low luminosity AGN or an ultraluminous X-ray source (Soria & Motch 2004).

In this letter we describe new observations of NGC 7714 with the *Spitzer Space Telescope*. These observations are part of an IRS guaranteed time program to obtain high signal-to-noise spectra of a large sample of different classes of nearby galaxies, that can be used for comparison with more distant systems (Devost et al. 2004, Higdon et al. 2004a, Houck et al. 2004a).

2. OBSERVATIONS AND DATA REDUCTION

We observed NGC 7714 with the Infrared Spectrograph (*IRS*) (Houck et al. 2004b) on board the *Spitzer Space Telescope* (Werner et al. 2004). The observations are part of the *IRS* guaranteed time program. The data were taken during the first *IRS* campaign in nominal operations on 17 December 2003 using the standard

Electronic address: brandl@strw.leidenuniv.nl
‡ Chercheur Associé, Observatoire de Paris, F-75014, Paris, France
[1] The *IRS* was a collaborative venture between Cornell University and Ball Aerospace Corporation funded by NASA through the Jet Propulsion Laboratory and the Ames Research Center.
[2] We adopt $H_0 = 71\,\mathrm{km\,s^{-1}\ Mpc^{-1}}, \Omega_\mathrm{M} = 0.27, \Omega_\Lambda = 0.73$

IRS "Staring Mode" Astronomical Observing Template (AOT). The dataset consists of observations with all four IRS modules: 2 cycles × 14s in "Short-low" (SL, $\Delta\lambda = 5.2 - 14.5\mu$m, $R \sim 64 - 128$), 2 cycles × 14s in "Long-low" (LL, $\Delta\lambda = 14.0 - 38.0\mu$m, $R \sim 64 - 128$), 4 cycles × 30s in "Short-high" (SH, $\Delta\lambda = 9.9 - 19.6\mu$m, $R \sim 600$), and 2 cycles × 60s in "Long-high" (LH, $\Delta\lambda = 18.7 - 37.2\mu$m, $R \sim 600$). Each cycle yields two exposures at different nod positions along the slit. The slits were positioned relative to the reference star SAO 128273 using an "IRS high accuracy peak-up" in the blue filter band.

The data have been pre-processed by the Spitzer Science Center (SSC) data reduction pipeline version 9.5 (Spitzer Observer's Manual, chapter 7[3]). The two-dimensional "basic calibrated data" (BCD) constituted the basis for further processing. The BCD frames have been individually inspected by eye, and hot pixels, as well as very negative pixels, that have not already been flagged by the pipeline, were masked manually. The former could easily be identified by flipping between images at different nod positions. Tests have shown that masked pixels introduce artificially high noise in the spectra, and hence we interpolated isolated masked pixels by their nearest neighbor pixel values along the dispersion direction. Next we averaged the frames from the same nod positions (in the case of SH where four frames per nod position were available we have used the median instead). Since the low-resolution, long-slit modules contain two sub-slits, each integration provides a "free" sky spectrum – mainly zodiacal emission – in the adjacent subslit. We computed the median sky and subtracted it from the low-resolution frames.

Further processing was done within the *IRS* data reduction and analysis package *SMART*, version v.4 (Higdon et al. 2004b) – a powerful IDL package for spectral extraction and spectral analysis. The high-resolution spectra were extracted with "full aperture" extraction along the diffraction orders. The ends of each orders where the noise increases significantly were manually clipped. Within any one module the individual orders matched remarkably well and required no further fine-tuning, with the exception of SH order 11 which was scaled up by 5%. Finally the two nod positions were averaged. The low-resolution spectra were extracted using *SMART*'s "interactive column extraction", which is similar to the method used in the SSC pipeline. The 3rd "bonus" order in SL and LL has not been included.

At the current stage of calibration, there remains a significant mismatch between some modules in both low- and high-resolution spectra. This mismatch is most likely due to either *(i)* extended source emission (as seen e.g. by O'Halloran et al. (2004)), or *(ii)* pointing errors that lead to flux losses that are most significant at short wavelengths (narrow slits). We also note that the low-resolution slits are narrower than the slits of the high-resolution modules. At this early stage of the Spitzer mission we have no means to identify the real cause. However, the LH and LL spectra agree very well with each other, and a comparison between the *IRAS* 25μm flux of 3.15 Jy (Surace et al. 2004) and the LL flux in the *IRAS* filterband of 2.61 Jy yields good agreement, taking into account that the *IRAS* "aperture" is much bigger and is even more susceptible to extended emission. Adopting the LH flux densities as correct, we scaled SH up by 36% to achieve an excellent match of the continuum fluxes around 19μm. We note that the flux in the [S III] line, which lies in the overlap region between SH and LH, is then the same in both modules. Similarly, the low-resolution spectra from different modules had to be scaled to match. The LL 2nd order was scaled up by 17% to match the LL 1st order; the SL 2nd order was scaled up by 40% to match the SL 1st order; and finally the resulting SL spectrum was scaled up by 17% to match the LL spectrum. As a result of this approach the low- and high resolution spectra agree very well with each other, and – even more important – we determine from the low-resolution spectrum in the *IRAS* 12μm band a total flux of 0.47 Jy, while Surace et al. (2004) found 0.56 Jy from *IRAS* – again good agreement! Figures 1 and 2 show the final *IRS* high- and low-resolution spectra, respectively.

The properties of the ionic and molecular features were obtained from single Gaussian fits to the high- and low-resolution spectra within *SMART*; the results are listed in tables 1 and 2.

3. RESULTS

3.1. *The starburst properties of NGC 7714*

Based on optical and near-IR spectroscopy (Lançon et al. 2001), the *ISOCAM* filter band ratios and PAH emission features (O'Halloran et al. 2004), it has long been argued that the nucleus of NGC 7714 is a site of intense starburst activity. However, given its low extinction, the unusually high infrared luminosity and recent reports of a possible, hidden AGN (Soria & Motch 2004) more precise diagnostics are needed to understand the processes in the nuclear region. The high signal-to-noise mid-IR *IRS* spectra provide the ideal diagnostic tools to characterize the nature of the underlying power source in more detail.

Table 1 lists the properties of the strongest fine-structure lines in the high-resolution spectrum (fig. 1). We find 10.8×10^{-20}Wcm^{-2} for the [Ne II] line while Phillips et al. (1984) found $(7 \pm 2) \times 10^{-20}$Wcm^{-2} from the ground. For the [S IV] line we determine 1.8×10^{-20}Wcm^{-2} while O'Halloran et al. (2004) quote $(3.2 \pm 0.8) \times 10^{-20}$ Wcm^{-2} based on *ISOPHOT-S* low-resolution spectra. The S(0), S(1), and S(2) lines of molecular hydrogen are marginally detected and will be discussed in a subsequent paper.

Of particular interest is the [Ne III] / [Ne II] ratio as it is a good measure of the hardness of the interstellar radiation field, which is mainly determined by the most massive stars. We find [Ne III] / [Ne II] $= 0.73 \pm 0.05$, corresponding to an effective temperature of about 3.8×10^4 K (Giveon et al. 2002). Based on the "*ISO-SWS* Starburst Sample", Thornley et al. (2000) studied the [Ne III] / [Ne II] ratio for 27 galaxies, with values ranging from 0.05 (M83) to 12.0 (II Zw 40), and a median value of 0.26. The starbursts of the nearby ISO sample with [Ne III] / [Ne II] ratios closest to our value are NGC 3690 (0.71) and the interaction region in NGC 4038/39 (0.84). The origin of these variations is still controversial (Rigby & Rieke 2004, Thornley et al. 2000). Even within the same galaxy the [Ne III] / [Ne II] ratio can vary significantly as recently seen with the *IRS* in NGC 253 (Devost

[3] http://ssc.spitzer.caltech.edu/documents/som/

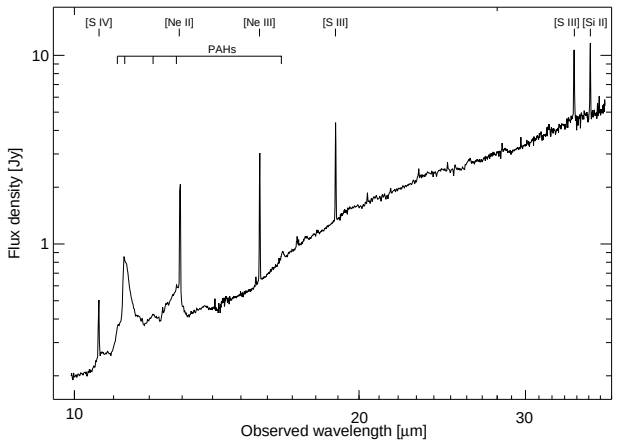

FIG. 1.— IRS high-resolution spectrum of NGC 7714. The total integration times are 240 seconds for both SH and LH (see discussion in the main text).

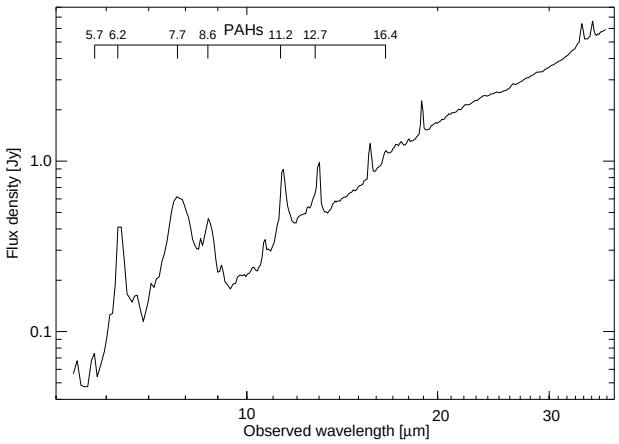

FIG. 2.— IRS low-resolution spectrum of NGC 7714 (see discussion in the main text). The total integration time is 56 seconds per subslit.

TABLE 1
FINE STRUCTURE LINES IN NGC 7714

ID	λ_{rest} [μm]	λ_{obs} [μm]	EP[a] [eV]	Flux[b] [10^{-20}Wcm^{-2}]	S/N[a]	EW[a] [μm]
[S IV]	10.51	10.61	34.8	1.79 ± 0.04	92	0.03
[Ne II]	12.81	12.94	21.6	10.82 ± 0.48	135	0.11
[Ne III]	15.56	15.63	41.0	7.95 ± 0.11	114	0.11
[S III]	18.71	18.89	23.3	9.01 ± 0.10	131	0.08
[S III]	33.48	33.77	23.3	12.61 ± 0.51	37	0.11
[Si II]	34.82	35.13	8.15	10.45 ± 0.36	48	0.09

NOTE. — Emission line properties obtained from a single Gaussian fit to the high-resolution data.

[a]EP = Excitation potential, EW = Equivalent width (observed), S/N = signal-to-noise ratio.

[b]The uncertainties quoted for the line fluxes throughout this letter are the errors from the line fit and do not include the calibration uncertainties.

TABLE 2
PAH EMISSION FEATURES IN NGC 7714

λ_{rest} [μm]	λ_{obs} [μm]	Flux [10^{-19}Wcm^{-2}]	EW [μm]	Relative strength[b]	Mod[a]
6.2	6.31	4.60 ± 0.44	0.50	0.49	lo
7.7	7.80	9.42 ± 0.39	0.70	1.00	lo
8.6	8.71	1.74 ± 0.28	0.17	0.18	lo
11.2	11.33	2.21 ± 0.28	0.17	0.23	hi
12.7	12.81	1.66 ± 0.16	0.14	0.18	hi
16.4	16.55	0.33 ± 0.03	0.03	0.04	lo

NOTE. — PAH band emission strength, For the measurement of the 12.7μm feature we first removed the [Ne II] line.

[a]lo = fit to low-resolution data, hi = fit to high-resolution data

[b]Relative to the 7.7μm feature.

et al. 2004). We will address this important issue in a subsequent paper once we have observed a larger sample of starburst galaxies. However, with its large number of very luminous Wolf-Rayet stars, it is not surprising that the [Ne III] / [Ne II] ratio in NGC 7714 lies above the value found in most starburst galaxies.

Although [O IV] has an excitation potential of 54.9 eV, faint emission has been seen in many starburst galaxies (Lutz et al. 1998) and recently with the *IRS* in the ultra-luminous IR-galaxy UGC 5101 (Armus et al. 2004). We also find a marginal detection of the [O IV] line with $(9.9 \pm 7.2) \times 10^{-21}$ Wcm^{-2}. Since the location of the line coincides with a noisy pixel, we take this value as an upper limit. Hence, with [O IV] / [Ne II] ≤ 0.09 and a relative PAH(7.7μm) / continuum(7.7μm) ≈ 1.30, NGC 7714 falls below the region occupied by ULIRGs in fig. 5 of Genzel et al. (1998). Furthermore, the absence of the [Ne V] line – we place a 3σ upper limit of 3.9×10^{-21} Wcm^{-2} – emphasizes the pure starburst nature of NGC 7714. On the basis of the infrared emission lines, therefore, we find no evidence for an obscured ionized region associated with an AGN, which implies that the variable X-ray source reported by Soria & Motch (2004) is either from strong shocks associated with very recent supernova activity, or emission from a HMXB. There is growing evidence that both possibilities are intimately associated with massive young star clusters (Gao et al. 2003).

3.2. *The dominant PAH features*

Below 13μm, the spectra are dominated by strong emission from PAHs (see e.g. Peeters et al. (2003) for a recent overview), with the strongest at 6.2μm, 7.7μm, 8.6μm, 11.2μm, 12.7μm, and 16.4μm listed in table 2. More features (e.g. at 5.7μm) appear to be present but will not be discussed here. Some of those features have also been seen in the *ISOPHOT-S* spectra which covered the $5-12\mu$m range at a resolution of $R = 90$ (O'Halloran et al. 2004). The total flux we determine for the strongest feature at 7.7μm agrees with the *ISOPHOT-S* measurement of $(8.84 \pm 1.10) \times 10^{-19}$ Wcm^{-2}.

Shortward of 13μm the spectrum is qualitatively very similar to the well-know starburst galaxy M82. However, unlike M82, which has very strong PAH emission with respect to the warm continuum from very small grains and plausibly some extinction due to silicates at 9.7μm (Förster-Schreiber et al. 2003), the spectrum of NGC 7714 shows a rather smooth continuum and no evidence for silicate absorption.

With the high signal-to-noise provided by *Spitzer-IRS* it now becomes possible to expand the comprehensive

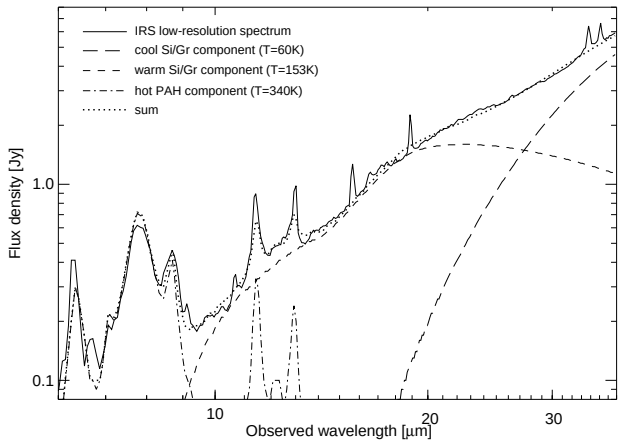

FIG. 3.— IRS low-resolution spectrum of NGC 7714 with the various fit components overlaid (see discussion in the text). Strong emission lines were excluded from the fit.

study of fainter PAH features seen in Galactic sources to a large sample of extragalactic sources. While the strength of e.g. the 6.2μm PAH / continuum ratio is remarkably constant over a wide luminosity range in Galactic sources, others, e.g. the 11.2μm feature, which is linked to neutral PAHs, get quickly reduced in stronger ionizing radiation fields (Hony et al. 2001).

Hony et al. (2001) show that the 12.7μm band correlates well with the CC stretch mode at 6.2μm for Galactic sources ranging from YSOs, H II regions, and reflection nebulae to planetary nebulae (their fig. 5). With $\log_{10}(I_{6.2}/I_{11.2}) = 0.32$ and $\log_{10}(I_{12.7}/I_{11.2}) = -0.12$, NGC 7714 falls right on their correlation line. We conclude that the physical conditions in NGC 7714 are similar to Galactic H II regions. In fact, a comparison with the *ISO-SWS* spectrum of M17 (Peeters et al. 2004) yields a perfect overall match longward of 15μm.

3.3. *Dust and Extinction in NGC 7714*

One of the most remarkable attributes in Figure 2 is the lack of silicate absorption in NGC 7714. This implies that the observed spectral shape of the mid-IR continuum is defined purely by the continuum emission of the hottest dust directly heated by the young, massive stars. If so then NGC 7714 might be a well-needed template for fitting relatively unobscured starbursts at low and high redshifts. Is NGC 7714 the perfect, unobscured starburst?

From the hydrogen recombination lines Paβ, Brγ, and Brα, Puxley & Brand (1994) determined $A_V = 1.8 \pm 0.7$ mag for a point source model with obscuring screen, and $A_V = 3.9 \pm 1.7$ mag if sources and dust are homogeneously mixed. For an extinction law of $A_{9.6\mu m}/A_V = 0.1$ and if $A_V = 3.9$ we find that $\tau_{9.6\mu m} = 0.36$ and hence the continuum around 9.6μm would be suppressed by a factor of at most 30%. In the case of an obscuring screen, which was favored by Puxley & Brand (1994), the suppression is only 15%, which is in good agreement with the shape of our spectrum.

The long wavelength baseline available in our spectrum of NGC 7714 makes possible a very accurate determination of the continuum, which allows sophisticated fits for the dust emission which is responsible for this continuum. Figure 3 shows a three component fit to the low-resolution spectrum. Two components are warm and cool astronomical silicate/graphite (Si/Gr) dust with an MRN distribution (Mathis et al. 1977) and the optical constants given by Draine & Lee (1984) and Laor & Draine (1993). The third component is astronomical PAHs for which we use the absorption coefficient of Siebenmorgen et al. (2001). We also allowed for the possibility of an intervening, absorbing Si/Gr dust screen but found that $\tau_{9.7\mu m} \leq 0.2$ (consistent with the above results). The Si/Gr dust components have temperatures of approximately 153 K and 60 K, and the PAH component has a temperature of about 340 K. PAH emission clearly dominates below 9μm while the Si/Gr mix fills in the "PAH trough" at 10.5μm. The Si/Gr component then dominates at longer wavelengths. A warm and a hot component are clearly present in NGC 7714. Due to the absence of silicate absorption, we have confidence that the continuum is directly observed, without being obscured by cooler, intervening dust. This means that we have achieved a direct measurement of the hottest dust in a prototypical galaxy. This determination is important because the dust temperature is often used as a discriminant between starbursts and AGN.

This work is based [in part] on observations made with the Spitzer Space Telescope, which is operated by the Jet Propulsion Laboratory, California Institute of Technology under NASA contract 1407. Support for this work was provided by NASA through Contract Number 1257184 issued by JPL/Caltech.

REFERENCES

Armus, L. et al., 2004, ApJS, this volume
Devost, D. et al., 2004, ApJS, this volume
Draine, B. T., & Lee, H. M., 1984, ApJ, 285, 89
Förster-Schreiber, N. M. et al., 2003, A&A, 399, 833
Gao, Y., Wang, Q. D., Appleton, P. N., Lucas, R. A.,2003, ApJL, 596, L171
Garcia-Vargas et al., 1997, ApJ, 478, 112
Genzel, R., et al., 1998, ApJ, 498, 579
Giveon, U., et al., 2002, ApJ, 566, 880
González-Delgado et al., 1995, ApJ, 439, 604
Higdon, S. J. U., et al., 2004a, ApJS, this volume
Higdon, S. J. U., et al., 2004b, PASP, submitted
Hony, S. et al., 2001, A&A, 370, 1030
Houck, J. R. et al., 2004a, ApJS, this volume
Houck, J. R. et al., 2004b, ApJS, this volume
Lançon, A. et al., 2001, ApJ, 552, 150
Laor, A., & Draine, B. T., 1993, ApJ, 402, 441
Lutz, D., Kunze, D., Spoon, H. W. W., Thornley, M. D., 1998, A&A, 333, L75
Mathis, J. S., Rumpl, W., Nordsieck, K. H., 1977, ApJ, 217, 425
O'Halloran, B. et al., 2000, A&A, 360, 871
Peeters, E. et al., 2002, A&A, 390, 1089
Peeters, E. et al., 2003, astro-ph/0312184
Peeters, E., Tielens, A.G.G.M., Spoon, H.W.W., 2004, in preparation
Phillips, M. M., Aitken, D. K. & Roche, P. F., 1984, MNRAS, 207, 25
Puxley, P. J. & Brand, P. W. J. L. 1994, MNRAS, 266, 431

Rigby, J. R. & Rieke, G. H., astro-ph/0401239, submitted to ApJ
Sanders, D. B., Scoville, N. Z. & Soifer, B. T., 1991, ApJ, 370, 158
Siebenmorgen, R., Krugel, E., Laureijs, R. J., 2001, A&A, 377, 735
Soria, R. & Motch, C., 2004, astro-ph/0402332
Struck, C. & Smith, B. J., 2003, ApJ, 589, 157
Sturm, E. et al., 2000, A&A, 358, 481
Surace, J, Mazzarella, J. M., Sanders, D. B., 2004, astro-ph/0402531
Taniguchi, Y. et al., 1988, AJ, 95, 1378
Thornley, M. D. et al., 2000, ApJ, 539, 641
Weedman, D. W. et al., ApJ, 248, 105
Werner, M. et al., 2004, "The Spitzer Space Telescope Mission", ApJS, this volume